
Evidence of Cyclic Changes in the Metabolism of Abdominal Aortic Aneurysms During Growth Phases: ^{18}F -FDG PET Sequential Observational Study

Olivier Morel¹⁻³, Damien Mandry²⁻⁴, Emilien Micard^{2,3}, Claude Kauffmann⁵, Zohra Lamiral⁶, Antoine Verger¹⁻³, Elodie Chevalier-Mathias^{1,7}, Julien Mathias⁴, Gilles Karcher¹⁻³, Benoit Meneroux¹, Patrick Rossignol^{3,6,7}, and Pierre-Yves Marie^{1,3,7}

¹Nuclear Medicine & Nancyclotep Experimental Imaging Platform, CHU Nancy, Nancy, France; ²UMR 947, INSERM, Nancy, France; ³Faculty of Medicine, University of Lorraine, Nancy, France; ⁴Department of Radiology, CHU Nancy, Nancy, France; ⁵LCTI, Université de Montréal, Montréal, Québec, Canada; ⁶Centre d'Investigation Clinique CIC-P 9501, INSERM, Nancy, France; and ⁷UMR 1116, INSERM, Nancy, France

The rates of growth of medically treated abdominal aortic aneurysms (AAA) are difficult to determine, and relationships with parietal inflammation and with metabolic parameters from ^{18}F -FDG PET remain unclear. This ^{18}F -FDG PET sequential observational study was aimed at analyzing the metabolic changes accompanying the growth phases of medically treated AAA. **Methods:** Thirty-nine patients (37 men; age [mean \pm SD], 71 \pm 12 y) exhibiting small and medically treated AAA (maximal diameter, 46 \pm 3 mm) underwent ^{18}F -FDG PET and CT angiography at baseline and 9 mo later. Clinical and imaging parameter correlates of the 9-mo increase in maximal diameter were investigated; these included ^{18}F -FDG maximal standardized uptake values (SUV_{max}) averaged for slices encompassing the AAA volume. **Results:** Of the 39 patients, 9 (23%) had a significant (≥ 2.5 mm) increase in maximal diameter at 9 mo, whereas the remaining 30 did not. The patients with an increase in maximal diameter at 9 mo exhibited lower SUV_{max} within the AAA at baseline than patients who did not have such an increase (1.80 \pm 0.45 vs. 2.21 \pm 0.52; $P = 0.04$); they also displayed a trend toward greater changes in SUV_{max} at 9 mo (difference between 9 mo and baseline: +0.40 \pm 0.85 vs. -0.06 \pm 0.57; $P = 0.07$). Similar levels were ultimately reached in both groups at 9 mo (2.20 \pm 0.83 and 2.15 \pm 0.66). SUV_{max} was a significant, yet modest, baseline predictor of the absolute change in maximal diameter during follow-up ($P = 0.049$). **Conclusion:** The enhancement in the maximal diameter of small AAA was preceded by a stage with a low level of ^{18}F -FDG uptake, but this low level of uptake was no longer documented after the growth phases, suggesting a pattern of cyclic metabolic changes.

Key Words: abdominal aortic aneurysms; maximal diameter; CT angiography; PET; ^{18}F -FDG

J Nucl Med 2015; 56:1030-1035

DOI: 10.2967/jnumed.114.146415

The prevalence of abdominal aortic aneurysms (AAA) remains high worldwide, affecting approximately 5% of elderly men (1). For most AAA, which are small and uncomplicated, only a periodic follow-up of the maximal diameter is required (1)—even if such screening is not sufficient to accurately determine the rupture risk at the individual level (2). Small AAA can rupture at nonnegligible rates of approximately 1% per year (3), whereas many AAA can grow to dramatic sizes without rupturing.

However, diameter-based screening is still important because large randomized trials have shown that survival is not improved by prophylactic surgery until a maximal diameter of 5.5 cm is reached (4). Additionally, enhanced risk is observed when increase rates are greater than or equal to 2 mm/y (5).

Several recent reports suggested that ^{18}F -FDG PET imaging has the potential to aid in risk stratification for AAA. In particular, the increased ^{18}F -FDG uptake in the AAA wall corresponds locally to macrophage infiltration and to enhanced proteolysis (6-9), 2 parameters having major roles in the growth and rupture of AAA (10). This increased uptake is also frequently documented when there is an obvious need for rapid surgical repair, such as for a symptomatic or rapidly expanding AAA (9,11).

In contrast, an abnormally low level of ^{18}F -FDG uptake is commonly documented for uncomplicated AAA (12,13), presumably because of a decrease in cellular density (8,13). Furthermore, the level of uptake may be even lower in AAA that are more likely to exhibit a subsequent enhancement in maximal diameter (14). During the growth phases, however, how this ^{18}F -FDG uptake evolves along with the metabolism and inflammation of AAA walls is unknown.

This ^{18}F -FDG PET sequential observational study was aimed at analyzing the metabolic changes accompanying the growth phases of medically treated AAA.

MATERIALS AND METHODS

Patient Selection and Study Design

The study protocol was approved by the local ethics committee (Comité de Protection des Personnes agreement 06.11.02) and released on the ClinicalTrials.gov website under the identifier NCT02182908.

All study patients gave signed informed consent to participate and were prospectively included if they met the following criteria: presence

Received Jul. 30, 2014; revision accepted Jan. 5, 2015.

For correspondence or reprints contact: Olivier Morel, Service de Médecine Nucléaire, CHU de Nancy—Hôpital de Brabois, Rue du Morvan, F-54500 Vandoeuvre, France.

E-mail: o.morel@chu-nancy.fr

Published online Mar. 19, 2015.

COPYRIGHT © 2015 by the Society of Nuclear Medicine and Molecular Imaging, Inc.

of an infrarenal AAA of a common atherosclerotic origin and for which only medical therapy was required (a criterion that implies the exclusion of symptomatic AAA and AAA with a maximal diameter of ≥ 55 mm), AAA maximal diameter of greater than or equal to 40 mm at CT angiography, age of greater than 18 y, no contraindication for ^{18}F -FDG PET or CT angiography, no antiinflammatory or immunosuppressant treatment, and no known disease that could lead to a marked inflammatory response.

The study patients were referred for baseline ^{18}F -FDG PET, which needed to be performed no later than 15 d after the initial CT angiography, and for a control assessment that was scheduled to be performed 9 mo (± 15 d) from the initial CT angiography and that involved additional ^{18}F -FDG PET and CT angiography. On the days on which baseline ^{18}F -FDG PET and control ^{18}F -FDG PET were performed, the patients underwent a medical assessment with blood pressure measurement.

Hybrid PET/CT Recording

^{18}F -FDG PET images were recorded on a Biograph hybrid system with 6-detector CT for attenuation correction and anatomic localization (Biograph 6 True Point; Siemens) (15,16). An ^{18}F -FDG activity of 5.5 MBq/kg was injected intravenously after an overnight fast. The blood glucose level had been previously verified with a dedicated electronic device so as to ensure a level of less than $1.5 \text{ g}\cdot\text{L}^{-1}$ in all patients. CT imaging was initiated 90 min later and was immediately followed by a 3-dimensional PET recording with 3 or 4 bed positions of 7 min each; all patients were scanned from the apex of the lungs to the iliac bifurcation.

The main CT parameters were as follows: 130 kV, intensity adapted to noise index, 512×512 matrix, 2-mm slice thickness, and pitch of 1. ^{18}F -FDG PET images were reconstructed by the ordered-subset expectation maximization method (3 iterations and 8 subsets) with corrections for scatter and attenuation and were subsequently displayed in a 128×128 matrix with $3.0 \times 3.0 \times 3.0$ mm voxels. The standardized uptake value (SUV) was calculated by dividing the activity measured in each voxel by the total injected activity expressed per gram of body weight and corrected for radioactive decay.

CT Angiography Recording

Images of the AAA were recorded during breath-hold periods of about 10 s on a 64-detector CT scanner (LightSpeed VCT; GE Healthcare). A total iodinated contrast volume of 1.5–2 mL/kg, with an iodine concentration of 300–400 mg/mL, was injected in an upper-limb vein at a rate of 3–5 mL/s; next, 20–60 mL of saline physiologic solution was injected at the same rate. Acquisition was triggered by bolus-tracking software. The main CT parameters were as follows: craniocaudal recording direction; 100–140 kV, depending on the patient's morphology; intensity adapted to noise index; rotation time of 0.6 s; pitch close to 1; 0.625-mm slice thickness; 512×512 matrix; and field of view adapted to the patient.

Analysis of Hybrid PET/CT Images

^{18}F -FDG PET images were analyzed with a paired display of both CT and fused PET/CT images provided by an Esoft station (Siemens) (15,16). The averaged values of aortic activities were quantified on consecutive transaxial slices encompassing the abdominal aorta. On each slice, a region of interest was drawn around the aorta, including the aneurysm wall and content, to allow the maximal ^{18}F -FDG uptake to be collected (maximal SUVs [SUV_{max}]). The values were averaged for slices covering the suprarenal abdominal aorta and the aneurysmal volume, with the exclusion of inferior and superior extremities (at a distance of 1 cm from each neck region). The averaged SUV_{max} was also divided by the mean blood voxel activity, estimated from the inferior vena cava, to provide maximal tissue-to-background ratios (17).

Analysis of CT Angiography

The maximal diameters of the AAA as well as diameter changes at 9 mo were determined with dedicated software, allowing a side-by-side display and reorientation of both baseline and 9-mo CT angiography studies (Volume Viewer; GE Healthcare). This analysis was performed separately and in a masked fashion by 2 experienced observers in accordance with current recommendations (delimitation of the external parietal limits after careful orientation, perpendicular to the long axis of the aneurysm long axis (18)). The maximal diameters measured by the 2 observers were subsequently averaged for further analyses, except when the difference was greater than 3 mm; in such cases, an additional and consensual determination was obtained from the 2 observers.

For assessment of the reproducibility of this process, maximal diameters were determined a second time from 36 CT angiography studies, and the mean \pm SD of the differences between the 2 determinations was calculated. Thereafter, the corresponding limits of agreement were used to define the cutoff value for significant changes in maximal diameter between baseline and 9 mo.

In addition, the total volume of the AAA as well as the volumes of the lumen and thrombus portions of the AAA were evaluated with A3Dmax segmentation software (Object Research System) (19). This software enables the segmentation and 3-dimensional modeling of the lumen and thrombus volumes of the AAA after the manual placement of upper- and lower-limit planes. In the present study, these limit planes were placed at the levels of the inferior renal artery and the aortoiliac bifurcation.

Statistical Analysis

Discrete variables were expressed as percentages, and continuous variables were expressed as mean \pm SD. Patients with a significant increase in the maximal diameter between baseline and 9 mo were defined as those for whom this difference exceeded the limits of agreement that were documented in the reproducibility analysis (upper limit of the 95% confidence interval). Mann–Whitney tests were used for 2-group comparisons of continuous variables, and Fisher exact tests were used for 2-group comparisons of discrete variables.

Wilcoxon signed rank tests were used for paired comparisons of continuous variables between baseline and 9 mo, the McNemar test was used for discrete variables, and the Spearman rank correlation coefficient method was used for determining the correlates of the differences in maximal diameter and volume of AAA between 9 mo and baseline. These correlates were investigated for baseline values only for CT angiography parameters and for both baseline and 9-mo values for the remaining parameters (Table 1).

For all tests, a *P* value of less than 0.05 was considered to indicate statistical significance.

RESULTS

A total of 51 patients were initially included and completed the baseline investigations. However, 12 patients were subsequently excluded, 1 because of a problem in the recording of ^{18}F -FDG PET images and 11 because of the lack of 9-mo investigations (7 patient refusals, 2 early referrals to AAA surgery, 1 allergy to iodinated contrast material, and 1 referral to carotid surgery at the time of the 9-mo investigations). Thus, 39 patients completed the overall protocol and constituted the final study population.

Baseline Data

The mean age of the 39 patients was 71 y (SD, 12 y; range, 38–88 y). Only 2 patients (5%) were women, and 24 (62%) had a history of cardiovascular disease (stroke in 2, coronary artery disease in 15, and peripheral arterial obstructive disease of the

TABLE 1
Paired Comparisons of Main Recorded Variables at Baseline and 9 Months (Control) (*n* = 39)

Variable	Baseline*	9 Mo*	<i>P</i>
Active smoking	8 (21)	10 (26)	NS
Body mass index (kg·m ²) [†]	28 ± 5	28 ± 5	NS
Systolic BP (mm Hg) [†]	141 ± 20	143 ± 18	NS
Diastolic BP (mm Hg) [†]	87 ± 11	87 ± 9	NS
Glycemia (mmol·L ⁻¹) [†]	4.66 ± 1.04	4.38 ± 0.86	NS
Insulinemia (mU·L ⁻¹) [†]	4.53 ± 2.48	3.69 ± 1.83	NS
Main medications			
Statins	28 (72)	30 (74)	NS
ACEI	20 (51)	19 (48)	NS
ARA II	9 (23)	9 (23)	NS
PAI	32 (82)	30 (75)	NS
Vitamin K antagonists	7 (18)	7 (18)	NS
CT parameters [†]			
Maximal diameter	46.0 ± 3.4	47.5 ± 4.2	<0.001
Volume of AAA (cm ³)	101 ± 21	110 ± 26	<0.001
Thrombus volume (cm ³)	40 ± 25	47 ± 31	<0.001
Lumen volume (cm ³)	62 ± 18	64 ± 19	0.02
¹⁸ F-FDG PET parameters [†]			
SUV _{max} of AAA	2.12 ± 0.53	2.17 ± 0.69	NS
TBR _{max} of AAA	1.55 ± 0.28	1.65 ± 0.43	NS
SUV _{max} of SRA	2.32 ± 0.58	2.30 ± 0.70	NS
TBR _{max} of SRA	1.69 ± 0.31	1.74 ± 0.32	NS

*Values are reported as number (percentage) of patients unless otherwise indicated.

[†]Values are reported as mean ± SD.

NS = not significant; BP = blood pressure; ACEI = angiotensin-converting enzyme inhibitor; ARA II = angiotensin II receptor antagonists; PAI = platelet aggregation inhibitors; TBR_{max} = maximal tissue-to-background ratio; SRA = suprarenal abdominal aorta.

lower limbs in 12). All but 2 (95%) had a history of smoking, 22 (56%) were treated for hypertension, and 5 (13%) were treated for diabetes.

Additional baseline characteristics are shown in Table 1. At CT angiography, the average maximal diameter of the AAA was 46 mm (SD, 3 mm; range, 40–54 mm), and the mean AAA volume was 101 mL (SD, 21 mL), including a thrombus volume of 40 mL (SD, 25 mL). At ¹⁸F-FDG PET, the mean SUV_{max} of the AAA was 2.1 (SD, 0.5), significantly lower than that of the suprarenal abdominal aorta (2.3 ± 0.6; *P* < 0.001). The mean SUV_{max} was unrelated to AAA diameter or volume. A high level of ¹⁸F-FDG uptake, which was easily detectable within the AAA, was a rare finding; a segment with an SUV_{max} of greater than or equal to 3 was documented in only 4 patients.

Evolution at 9 Months

As shown in Table 1, there was no significant difference between the baseline and the 9-mo control for all analyzed clinical and blood parameters.

There were significant enhancements at 9 mo for all CT parameters as opposed to none for ¹⁸F-FDG PET parameters (Table 1). In particular, the maximal diameter of the AAA was increased at 9 mo, with a mean difference from the baseline of 1.4 mm (SD, 1.9 mm). However, this difference was greater than or equal to 2.5 mm and

considered to be significant in only 9 patients, who were placed in a group designated D+ (i.e., those with a significant [≥2.5 mm] increase in maximal diameter at 9 mo), whereas the remaining 30 patients were placed in a group designated D– (i.e., those without such an increase). This threshold of 2.5 mm corresponded to the upper limit of the 95% confidence interval of the reproducibility analysis.

Correlates of Growth Rates at Baseline and at 9 Months

The sole baseline imaging parameters showing significant differences between D+ and D– patients were SUV_{max} within the AAA, which was lower in D+ patients, and AAA volume, which was higher in D+ patients (Table 2).

As shown in Table 2 and Figure 1, D+ patients exhibited lower SUV_{max} within the AAA at baseline than D– patients (1.80 ± 0.45 vs. 2.21 ± 0.52; *P* = 0.04); they also displayed a trend toward greater changes in SUV_{max} at 9 mo (difference between 9 mo and baseline: +0.40 ± 0.85 vs. –0.06 ± 0.57; *P* = 0.07). Similar levels were ultimately reached in both groups at 9 mo (2.20 ± 0.83 and 2.15 ± 0.66). The changes in SUV_{max} during the growth phases could be particularly striking, as shown in Figure 2.

D+ patients also had a lower mean SUV_{max} within the suprarenal aorta than D– patients, but the difference was not significant (2.01 ± 0.51 vs. 2.41 ± 0.57; *P* = 0.11).

TABLE 2

Comparison of Imaging Parameters for Patients With (D+) and Patients Without (D-) Increase in Maximal Diameter at 9 Months

Parameter	D+ group (n = 9)*	D- group (n = 30)*	P
Baseline CT parameters			
Maximal diameter	47.8 ± 3.3	45.5 ± 3.4	NS
Volume of AAA (cm ³)	113 ± 17	99 ± 22	0.03
Thrombus volume (cm ³)	46 ± 27	38 ± 25	NS
Lumen volume (cm ³)	67 ± 19	61 ± 18	NS
Evolution of ¹⁸F-FDG uptake			
SUV _{max} of AAA	1.80 ± 0.45	2.21 ± 0.52	0.04
Baseline			
9 mo	2.20 ± 0.83	2.15 ± 0.66	NS
Difference	0.40 ± 0.85	-0.06 ± 0.57	0.07
TBR _{max} of AAA	1.23 ± 0.19	1.28 ± 0.19	NS
Baseline			
9 mo	1.44 ± 0.42	1.31 ± 0.23	NS
Difference	0.21 ± 0.47	0.03 ± 0.23	NS
SUV _{max} of SRA	2.01 ± 0.51	2.41 ± 0.57	NS
Baseline			
9 mo	2.21 ± 0.35	2.33 ± 0.77	NS
Difference	0.20 ± 0.57	-0.08 ± 0.57	NS
TBR _{max} of SRA	1.75 ± 0.41	1.67 ± 0.28	NS
Baseline			
9 mo	1.85 ± 0.26	1.71 ± 0.33	NS
Difference	0.10 ± 0.45	0.04 ± 0.26	NS

*Values are reported as mean ± SD.

NS = not significant (P > 0.1); TBR_{max} = maximal tissue-to-background ratio; SRA = suprarenal abdominal aorta.

In addition, the difference in maximal diameter between 9 mo and baseline was slightly but significantly related to the baseline SUV_{max} of the AAA (P = 0.049) (Fig. 3). None of the other analyzed variables represented a significant predictor. However, trends toward greater differences in diameter were documented for patients who were still actively smoking at 9 mo (2.3 ± 2.7 mm for such patients vs. 1.2 ± 1.5 mm for other patients; P = 0.08) and for AAA with larger volumes at baseline (P = 0.07 for the analysis of the correlation between differences in diameter and AAA volume).

Finally, none of the baseline imaging parameters was predictive of the difference in AAA volume between baseline and 9 mo.

DISCUSSION

One of the key questions underlying the present study was whether ¹⁸F-FDG PET has the potential to aid in risk stratification for AAA. Indeed, on the one hand, increased ¹⁸F-FDG uptake within the AAA wall is correlated with macrophage infiltration and hyperproteolysis in situ (6–9). Furthermore, parietal ¹⁸F-FDG foci can be observed when AAA are prone to rupture and, more precisely, when they are large, rapidly expanding, or symptomatic (11). Such foci have yet to be documented at the actual site of rupture (9). However, on the other hand, focal or diffuse

increases in ¹⁸F-FDG uptake are likely to be a rare finding in patients with asymptomatic AAA, even when the maximal diameter is close to surgical indications (12,20). Surprisingly, an inverse

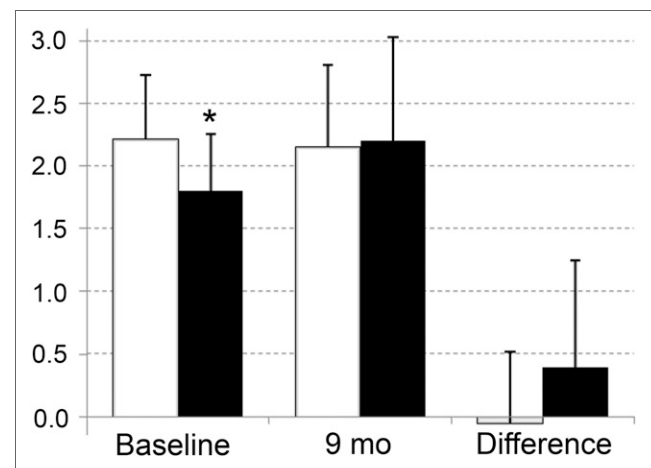


FIGURE 1. Comparison of 9-mo evolution of ¹⁸F-FDG activity within AAA (SUV_{max}) between patients with (■) and patients without (□) significant (≥2.5 mm) increase in maximal diameter during same period. *P < 0.05 for between-group comparisons.

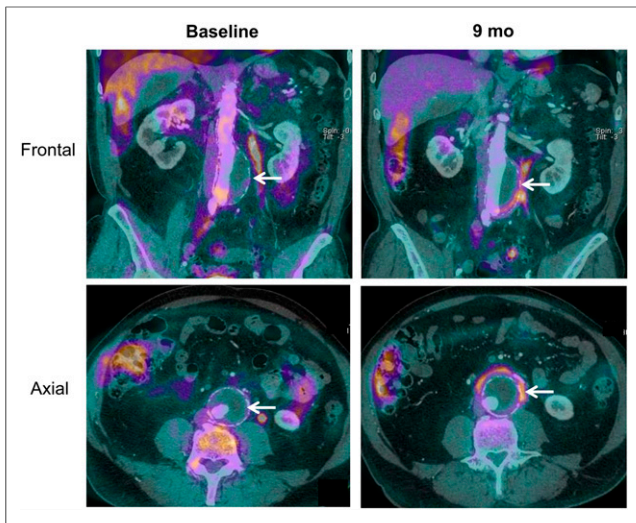


FIGURE 2. Frontal and axial fused images from ^{18}F -FDG PET and CT angiography showing marked enhancement in ^{18}F -FDG uptake (arrows) between baseline (SUV_{max} , 1.9) and 9 mo (control; SUV_{max} , 4.2) after growth phases of AAA (47 mm for maximal diameter at baseline and 57 mm at 9 mo). Area with enhanced ^{18}F -FDG uptake corresponds to thickening of presumably inflammatory tissue outside intimal calcifications on CT scan.

correlation between ^{18}F -FDG uptake and the subsequent rates of growth of asymptomatic AAA was recently documented (14).

These findings are further confirmed by the results of the present ^{18}F -FDG PET sequential observational study of patients with asymptomatic AAA considered to be below the threshold for surgical repair (46 ± 3 mm for baseline maximal diameter). First, the mean level of ^{18}F -FDG uptake, as determined with the SUV_{max} , was significantly lower than that documented in the suprarenal nondilated portion of the aorta, in accordance with previous observations (12,20). Second, an even lower level of ^{18}F -FDG uptake was documented at baseline in the AAA of the 9 patients for whom CT angiography yielded evidence of a subsequent increase in maximal diameter at 9 mo (control). Third, an inverse relationship was observed between baseline ^{18}F -FDG uptake and the absolute change in the maximal diameter at 9 mo (Fig. 3), in accordance with a previous observation (14).

Recent histopathologic studies showed that the low level of ^{18}F -FDG uptake of asymptomatic AAA reflects the metabolic activity of a small number of cells present within arterial walls (13), especially in fibrotic and necrotic regions (8). It is noteworthy that these cells include not only inflammatory cells but also smooth muscle cells exhibiting a sustained increase in glucose uptake, especially when stimulated and chronically exposed to inflammatory cytokines, a common situation within atherosclerotic walls (21,22).

Thus, in the atherosclerotic walls of most asymptomatic AAA, the overall number of cells able to entrap ^{18}F -FDG is considerably reduced, leading to a global low level of ^{18}F -FDG uptake (8,13,20). These data imply that, in such cases, chronic inflammation would not be sufficiently active to result in increased glucose metabolism detectable by PET cameras (20). From a technical imaging standpoint, such detection is also likely to be further impaired by partial-volume effects related to the thinness of arterial walls (7).

In the present study, as well as in the study by Kotze et al. (14), the level of ^{18}F -FDG uptake was found to be even lower in AAA that were more likely to exhibit a subsequent enhancement in max-

imal diameter. This inverse relationship was lost when ^{18}F -FDG uptake was assessed through the tissue-to-background ratio, similar to what was observed by Kotze et al. (14), presumably because this method of correcting for background activity is not well adapted to this setting. High and variable proportions of AAA walls are indeed covered by thrombus, in which activity is dramatically lower than in circulating blood. The activity documented in such thrombus-covered walls is likely to be minimally influenced by the level of ^{18}F -FDG in blood.

Figure 3 shows that a clear increase in maximal diameter was a rare finding in our study population, even for AAA exhibiting a low level of ^{18}F -FDG uptake at baseline. However, it must be kept in mind that AAA growth is likely to involve not only parietal but also important blood determinants. In particular, the thrombus of AAA is metabolically active, with variable production of cytokines and proteases that may influence the metabolism and structure of arterial walls (23).

On average, growth phases were found to be preceded by a stage of low metabolism, with a low level of ^{18}F -FDG uptake, but the main original observation of the present sequential study was the reversible nature of this stage. A trend toward greater changes in ^{18}F -FDG uptake was indeed documented in patients with an increased maximal diameter at 9 mo (Fig. 1); the uptake levels seen in the other patients at 9 mo (control) were ultimately reached.

These cyclic changes in ^{18}F -FDG uptake are in keeping with the cyclic inflammatory process of atherosclerosis development and with the transient nature of ^{18}F -FDG uptake within atherosclerotic lesions (24,25). These changes are also in accordance with the current model of AAA progression, which involves repetitive sequences of enlargement and inflammation (26,27). These cyclic changes are best illustrated in Figure 2, which shows a dramatic enhancement in ^{18}F -FDG uptake and in wall thickness after a growth phase, an observation similar to that previously documented in a case report (9). Such an enhancement in ^{18}F -FDG uptake may relate to the recruitment of additional inflammatory cells but also to the inflammation-related activation of smooth muscle cells (21,22).

An additional observation was that patients with an increased diameter at 9 mo showed a trend toward a lower level of ^{18}F -FDG uptake within the suprarenal aorta at baseline. Even if the difference between these patients and the other patients was not significant, this observation leads us to wonder to what extent these

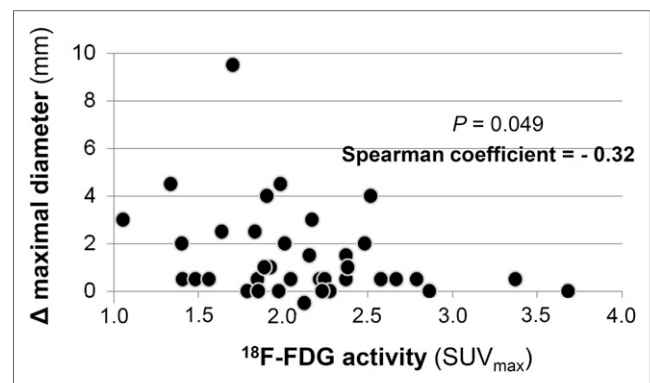


FIGURE 3. Relationship between difference (Δ) in maximal AAA diameter between baseline and 9 mo (control) and ^{18}F -FDG activity within AAA (SUV_{max}) at baseline.

metabolic changes are diffuse rather than strictly located within the AAA walls.

Taken together, these observations led us to consider that enhanced ^{18}F -FDG uptake, in relation to an enhanced inflammatory reaction, does not precede the growth phases of uncomplicated AAA, and we wonder whether enhanced ^{18}F -FDG uptake may accompany the growth phases. Only a trend toward enhanced ^{18}F -FDG uptake was documented here, together with an increase in the maximal diameter. However, our 9-mo delay was likely too long to image all inflammatory phases. On serial PET imaging from cancer patients, arterial ^{18}F -FDG foci were indeed found to normalize at a shorter and highly variable delay (6.8 ± 4.3 mo (25)). However, further studies with larger populations and higher imaging rates during follow-up are needed to clarify the relationship between growth phases and cyclic changes in ^{18}F -FDG uptake.

CONCLUSION

The present study showed that the enhancement in the maximal diameter of small AAA was preceded by a stage with a low level of ^{18}F -FDG uptake, but this low level of uptake was no longer documented after the growth phases, suggesting a pattern of cyclic metabolic changes. At the level of individual subjects, ^{18}F -FDG PET was not an effective tool for predicting the growth phases of small and asymptomatic AAA.

DISCLOSURE

The costs of publication of this article were defrayed in part by the payment of page charges. Therefore, and solely to indicate this fact, this article is hereby marked "advertisement" in accordance with 18 USC section 1734. This work was funded by a grant from the French Health Ministry (Programme Hospitalier de Recherche Clinique Inter-régional). The Nancyclotep Experimental Imaging Platform provided financial and organizational support. No other potential conflict of interest relevant to this article was reported.

ACKNOWLEDGMENT

We thank Pierre Pothier for critical review of the article.

REFERENCES

1. Guirguis-Blake JM, Beil TL, Senger CA, Whitlock EP. Ultrasonography screening for abdominal aortic aneurysms: a systematic evidence review for the U.S. Preventive Services Task Force. *Ann Intern Med.* 2014;160:321–329.
2. Brown LC, Powell JT. Risk factors for aneurysm rupture in patients kept under ultrasound surveillance: UK Small Aneurysm Trial Participants. *Ann Surg.* 1999;230:289–296.
3. Powell JT, Gotensparre SM, Sweeting MJ, Brown LC, Fowkes FG, Thompson SG. Rupture rates of small abdominal aortic aneurysms: a systematic review of the literature. *Eur J Vasc Endovasc Surg.* 2011;41:2–10.
4. United Kingdom Small Aneurysm Trial Participants. Long-term outcomes of immediate repair compared with surveillance of small abdominal aortic aneurysms. *N Engl J Med.* 2002;346:1445–1452.
5. Thompson AR, Cooper JA, Ashton HA, Hafez H. Growth rates of small abdominal aortic aneurysms correlate with clinical events. *Br J Surg.* 2010;97:37–44.
6. Reeps C, Essler M, Pelisek J, Seidl S, Eckstein HH, Krause BJ. Increased ^{18}F -fluorodeoxyglucose uptake in abdominal aortic aneurysms in positron emission/computed tomography is associated with inflammation, aortic wall instability, and acute symptoms. *J Vasc Surg.* 2008;48:417–423.
7. Reeps C, Bundschuh RA, Pellisek J, et al. Quantitative assessment of glucose metabolism in the vessel wall of abdominal aortic aneurysms: correlation with histology and role of partial volume correction. *Int J Cardiovasc Imaging.* 2013;29:505–512.
8. Courtois A, Nusgens BV, Hustinx R, et al. ^{18}F -FDG uptake assessed by PET/CT in abdominal aortic aneurysms is associated with cellular and molecular alterations prefacing wall deterioration and rupture. *J Nucl Med.* 2013;54:1740–1747.
9. Reeps C, Gee MW, Maier A, et al. Glucose metabolism in the vessel wall correlates with mechanical instability and inflammatory changes in a patient with a growing aneurysm of the abdominal aorta. *Circ Cardiovasc Imaging.* 2009;2:507–509.
10. Choke E, Cockerill G, Wilson WR, et al. A review of biological factors implicated in abdominal aortic aneurysm rupture. *Eur J Vasc Endovasc Surg.* 2005;30:227–244.
11. Sakalihasan N, Van Damme H, Gomez P, et al. Positron emission tomography (PET) evaluation of abdominal aortic aneurysm (AAA). *Eur J Vasc Endovasc Surg.* 2002;23:431–436.
12. Palombo D, Morbelli S, Spinella G, et al. A positron emission tomography/computed tomography (PET/CT) evaluation of asymptomatic abdominal aortic aneurysms: another point of view. *Ann Vasc Surg.* 2012;26:491–499.
13. Marini C, Morbelli S, Armonino R, et al. Direct relationship between cell density and FDG uptake in asymptomatic aortic aneurysm close to surgical threshold: an in vivo and in vitro study. *Eur J Nucl Med Mol Imaging.* 2012;39:91–101.
14. Kotze CW, Groves AM, Menezes LJ, et al. What is the relationship between ^{18}F -FDG aortic aneurysm uptake on PET/CT and future growth rate? *Eur J Nucl Med Mol Imaging.* 2011;38:1493–1499.
15. Mandry D, Tatopoulos A, Chevalier-Mathias E, et al. ^{18}F -fluorodeoxyglucose positron emission tomography combined with whole-body computed tomographic angiography in critically ill patients with suspected severe sepsis with no definite diagnosis. *Eur J Nucl Med Mol Imaging.* 2014;41:1924–1930.
16. Grandpierre S, Desandes E, Meneroux B, et al. Arterial foci of F-18 fluorodeoxyglucose are associated with an enhanced risk of subsequent ischemic stroke in cancer patients: a case-control pilot study. *Clin Nucl Med.* 2011;36:85–90.
17. Rudd JH, Myers KS, Bansilal S, et al. Atherosclerosis inflammation imaging with ^{18}F -FDG PET: carotid, iliac, and femoral uptake reproducibility, quantification methods, and recommendations. *J Nucl Med.* 2008;49:871–878.
18. Cayne NS, Veith FJ, Lipsitz EC, et al. Variability of maximal aortic aneurysm diameter measurements on CT scan: significance and methods to minimize. *J Vasc Surg.* 2004;39:811–815.
19. Kauffmann C, Tang A, Therasse E, et al. Measurements and detection of abdominal aortic aneurysm growth: accuracy and reproducibility of a segmentation software. *Eur J Radiol.* 2012;81:1688–1694.
20. Tegler G, Ericson K, Sörensen J, Björck M, Wanhainen A. Inflammation in the walls of asymptomatic abdominal aortic aneurysms is not associated with increased metabolic activity detectable by ^{18}F -fluorodeoxyglucose positron-emission tomography. *J Vasc Surg.* 2012;56:802–807.
21. Brammen L, Palumbo B, Lupattelli G, Sinzinger H. Is ^{18}F -FDG PET really a promising marker for clinically relevant atherosclerosis? *Hell J Nucl Med.* 2014;17:62–63.
22. Folco EJ, Sheikine Y, Rocha VZ, et al. Hypoxia but not inflammation augments glucose uptake in human macrophages: implications for imaging atherosclerosis with ^{18}F fluorine-labeled 2-deoxy-D-glucose positron emission tomography. *J Am Coll Cardiol.* 2011;58:603–614.
23. Michel JB, Martin-Ventura JL, Egado J, et al. FAD EU consortium: novel aspects of the pathogenesis of aneurysms of the abdominal aorta in humans. *Cardiovasc Res.* 2011;90:18–27.
24. Ben-Haim S, Kupzov E, Tamir A, Frenkel A, Israel O. Changing patterns of abnormal vascular wall F-18 fluorodeoxyglucose uptake on follow-up PET/CT studies. *J Nucl Cardiol.* 2006;13:791–800.
25. Menezes LJ, Kayani I, Ben-Haim S, Hutton B, Eli PJ, Groves AM. What is the natural history of ^{18}F -FDG uptake in arterial atheroma on PET/CT? Implications for imaging the vulnerable plaque. *Atherosclerosis.* 2010;211:136–140.
26. Kurvers H, Veith FJ, Lipsitz EC, et al. Discontinuous, staccato growth of abdominal aortic aneurysms. *J Am Coll Surg.* 2004;199:709–715.
27. Vega de Céniga M, Gómez R, Estallo L, de la Fuente N, Vivienis B, Barba A. Analysis of expansion patterns in 4–4.9 cm abdominal aortic aneurysms. *Ann Vasc Surg.* 2008;22:37–44.